Dendritic cells are crucial for maintenance of tertiary lymphoid structures in the lung of influenza virus–infected mice

Corine H. GeurtsvanKessel,[1,2] Monique A.M. Willart,[3] Ingrid M. Bergen,[1] Leonie S. van Rijt,[1,5] Femke Muskens,[1] Dirk Elewaut,[4] Albert D.M.E. Osterhaus,[2] Rudi Hendriks,[1] Guus F. Rimmelzwaan,[2] and Bart N. Lambrecht[1,3]

[1]Department of Pulmonary Medicine and [2]Department of Virology, Erasmus University Medical Center, Rotterdam 3000 CA, Netherlands
[3]Laboratory of Immunoregulation and Mucosal Immunology, Department of Respiratory Diseases, and [4]Laboratory of Molecular Immunology, University Ghent, Ghent B-9000, Belgium
[5]Department of Experimental Immunology, Academic Medical Center, University of Amsterdam, Amsterdam 1105 AZ, Netherlands

Tertiary lymphoid organs (TLOs) are organized aggregates of B and T cells formed in post-embryonic life in response to chronic immune responses to infectious agents or self-antigens. Although CD11c$^+$ dendritic cells (DCs) are consistently found in regions of TLO, their contribution to TLO organization has not been studied in detail. We found that CD11c^{hi} DCs are essential for the maintenance of inducible bronchus-associated lymphoid tissue (iBALT), a form of TLO induced in the lungs after influenza virus infection. Elimination of DCs after the virus had been cleared from the lung resulted in iBALT disintegration and reduction in germinal center (GC) reactions, which led to significantly reduced numbers of class-switched plasma cells in the lung and bone marrow and reduction in protective antiviral serum immunoglobulins. Mechanistically, DCs isolated from the lungs of mice with iBALT no longer presented viral antigens to T cells but were a source of lymphotoxin (LT) β and homeostatic chemokines (CXCL-12 and -13 and CCL-19 and -21) known to contribute to TLO organization. Like depletion of DCs, blockade of LTβ receptor signaling after virus clearance led to disintegration of iBALT and GC reactions. Together, our data reveal a previously unappreciated function of lung DCs in iBALT homeostasis and humoral immunity to influenza virus.

CORRESPONDENCE
Bart N. Lambrecht:
bart.lambrecht@ugent.be

Abbreviations used: BALf, bronchoalveolar lavage fluid; cDC, conventional DC; dpi, day post infection; DT, diphtheria toxin; DTR, DT receptor; FDC, follicular DC; GC, germinal center; HA, hemagglutinin; iBALT, inducible bronchus-associated lymphoid tissue; i.t., intratracheally; NP, nucleoprotein; SLO, secondary lymphoid organ; TLO, tertiary lymphoid organ.

The organized accumulation of lymphocytes in lymphoid organs serves to optimize both homeostatic immune surveillance and chronic responses to pathogenic stimuli (Cupedo and Mebius, 2005). During embryonic development, circulating hemopoietic cells gather at predestined sites throughout the body, where they are subsequently arranged in T and B cell–specific areas, which is characteristic of secondary lymphoid organs (SLOs). In contrast, the body seems to harbor a limited second set of selected sites that support neoformation of organized lymphoid aggregates in adult life. However, these are only revealed at times of local chronic inflammation when so-called tertiary lymphoid organs (TLOs) appear. As such, TLO was found in the pancreas of autoimmune diabetic mice (Kendall et al., 2007), around blood vessels in chronic allograft rejection (Nasr et al., 2007) and atherosclerosis (Gräbner et al., 2009), and in the brain in experimental allergic encephalitis (Magliozzi et al., 2004). In humans, TLO has been observed in the joint and lung of rheumatoid arthritis (Rangel-Moreno et al., 2006), around the airways of COPD patients (Hogg et al., 2004), and in the thyroid (Marinkovic et al., 2006). Certain infectious diseases are also accompanied by formation of TLO. Influenza

G.F. Rimmelzwaan and B.N. Lambrecht contributed equally to this paper.

The Rockefeller University Press $30.00
J. Exp. Med. Vol. 206 No. 11 2339-2349
www.jem.org/cgi/doi/10.1084/jem.20090410

The Journal of Experimental Medicine

virus infection of the respiratory tract leads to formation of inducible bronchus-associated lymphoid tissue (iBALT) that supports T and B cell proliferation and productive immunoglobulin class switching in germinal centers (GCs; Moyron-Quiroz et al., 2004, 2006).

Although the embryonic development of SLO requires $CD3^-CD4^+$ lymphoid tissue–inducer cells, these are not a prerequisite for TLO induction (Marinkovic et al., 2006; Rangel-Moreno et al., 2007). Like SLOs, TLOs are formed in a highly regulated manner via production of homeostatic chemokines (CXCL13 and CCL19/CCL21), partially in response to signaling from the heterotrimer lymphotoxin (LT) $\alpha_1\beta_2$ acting on the LTβ receptor on stromal lymphoid tissue organizer cells (Drayton et al., 2006). The instruction of stromal cells leads to formation of specialized high endothelial venules, and the organized production of chemokines leads to cellular organization of T cells and B cells in discrete areas. In all instances where TLOs have been described, antigen-presenting DCs have been found interspersed with T and B cell area, just as they are in SLO (Kratz et al., 1996; Cupedo et al., 2004; Moyron-Quiroz et al., 2004; Marinkovic et al., 2006; Tsuji et al., 2008). So far, the precise role of DCs in the functional organization of TLO has not been studied in great detail. Although DCs are mainly known for their function as antigen-presenting cells (Banchereau and Steinman, 1998), they are also a prominent source of homeostatic and inflammatory chemokines that can attract T and B cells and, thus, may contribute to TLO homeostasis (Beaty et al., 2007; GeurtsvanKessel and Lambrecht, 2008). In this paper, we have studied the precise contribution of DCs in the functional organization of iBALT, a specific form of TLO found in the lung after influenza virus infection (Moyron-Quiroz et al., 2004; Kocks et al., 2007).

RESULTS AND DISCUSSION

Lung $CD11c^+$ DCs localize to zones of iBALT after clearance of influenza virus

Mice were infected intranasally with a nonlethal strain of influenza A/HKX-31 (H3N2) that is cleared from the lungs at 8 d post infection (dpi; GeurtsvanKessel et al., 2008) and is accompanied by formation of iBALT as soon as 10 dpi. At various dpi, the presence of $CD11c^+$ DC subsets ($CD11b^+$ and $CD11b^-$) was determined in dispersed lung cells. In mock-infected mice, a majority of DCs were $CD11b^-$. Up to at least 24 dpi, the percentage of $CD11b^+CD11c^+$ DCs remained increased in influenza over mock-infected mice (Fig. 1 A; GeurtsvanKessel et al., 2008). $CD11c^+$ DCs were found within areas of $B220^+$ B cell aggregates, which were poorly delineated at 4 dpi but became progressively more organized into discrete lymphoid aggregates at 10 and 24 dpi (Fig. 1 B). The number of lung $CD11b^+CD11c^+$ DCs (Fig. 1 C) continued to rise after influenza infection, despite the fact that this virus is cleared from the lung at 8 dpi (GeurtsvanKessel et al., 2008). The rise in $CD11b^+$ DCs was accompanied by a rise in the percentage of lymphocytes recovered in lung cell suspensions (Fig. 1 D). At 17 dpi (Fig. 1 E), cell aggregates resembled iBALT and were characterized by a $B220^+$ B cell area containing some CD4 T cells, with a close-by T cell area containing DCs and CD4 and CD8 T cells. The B cell area contained follicular DC (FDC)–$M2^+$ FDCs and $PNAD^+$ high endothelial venules in the T cell area (not depicted; Rangel-Moreno et al., 2007). Although iBALT was mainly present in close proximity to bronchi, it was also seen in the lung interstitium.

Lung DCs are necessary for maintenance of iBALT after viral clearance

A CD11c diphteria toxin (DT) receptor (DTR) transgenic mouse model was used to deplete $CD11c^+$ DCs from the lungs, and thus study if these cells were necessary for maintenance of iBALT structures (GeurtsvanKessel et al., 2008). Mice received DT intratracheally (i.t.) at 17 dpi (Fig. 2 A). $CD11b^+CD11c^+$ DCs were depleted from the lung (Fig. 2 B) and draining mediastinal LN (Fig. S1 A) but not from the spleen or other SLOs (not depicted). $CD11c^{interm}$ plasmacytoid DCs were minimally affected by DT treatment (Sapoznikov et al., 2007). Although $CD11c^+$ IgM-producing extrafollicular plasmablasts were shown to be DT sensitive (Hebel et al., 2006), 24 h after DT treatment at 17 dpi, only $CD11c^+$ DCs were significantly depleted, whereas $CD4^+$ T cells, $CD8^+$ T cells, B cells, or $CD138^+$ plasma cells were not (Fig. S1 D). Staining for $F4/80^+$ cells also revealed insensitivity of iBALT macrophages to DT (unpublished data), although highly autofluorescent alveolar macrophages were depleted (van Rijt et al., 2005). 48 h after injection of DT, $CD11c^+$ DCs had disappeared from the iBALT structures, whereas $B220^+$ B cells were still abundantly present (Fig. 2 C). Although infected CD11c-DTR Tg mice treated with PBS (Fig. 2 C, top left) or nontransgenic mice treated with DT (not depicted) had extensive iBALT structures containing $B220^+$ B cells and $CD11c^+$ cells throughout the lung, these structures were significantly reduced after DT treatment of CD11c-DTR Tg mice (Fig. 2 C, right). Some $B220^+$ B cells were still detected in the lung tissue of DT-treated mice. Although some cells clustered into discrete regions, the density of B cells was strongly reduced and these regions no longer contained $CD11c^+$ cells (Fig. 2 C, insets). Histological quantification (Fig. 2 D) revealed a progressive decline in the number of iBALT per low-power field that was first evident 4 d after DC depletion and was almost complete by 1 wk after DC depletion, a time point when $CD11b^+CD11c^+$ DCs had already returned to the lungs of DT-treated mice (Fig. 2 B, bottom). The gradual disappearance of $B220^+$ cells and iBALT structures from the lungs, as opposed to the immediate disappearance of $CD11c^+$ DCs, is further proof that $B220^+$ B cells were not directly killed by DT treatment but were reduced secondary to DC depletion. This conclusion is supported by the observation that only 4% of lung B cells expressed CD11c.

DC depletion after viral clearance affects local humoral immune responses

The precise contribution of TLO to adaptive immunity is thought to serve local immune responses to microbial-derived

antigens or to autoantigens (Aloisi and Pujol-Borrell, 2006). Although a role for iBALT in mediating humoral immunity to influenza has been proposed, these studies were performed in mice lacking SLO through genetic manipulation (Moyron-Quiroz et al., 2006). The breakdown of iBALT in DC-depleted mice allowed us to study the functional contribution of these local structures to humoral immunity in mice with normal SLO. GC B cells undergoing active Ig class switching are typically found within TLO, including iBALT (Moyron-Quiroz et al., 2004). This is supported by the finding of FDCs within B cell regions (Fig. 1 E). Presence of GCs was demonstrated by staining consecutive slides for GL-7 (revealing GC B cells) and IgD (revealing mainly mantle B cells) and Ig isotypes (Fig. 3 A). In addition to IgD$^+$ B cells, class-switched plasma cells secreting IgG and IgA were found at the periphery of the iBALT. Similar conclusions were reached when GCs were identified using PNA staining, in which case IgM-secreting plasmablasts were also found (Fig. S2 A). We next addressed whether plasma cells were specific for influenza. For this purpose, recombinant nucleoprotein (NP) was used

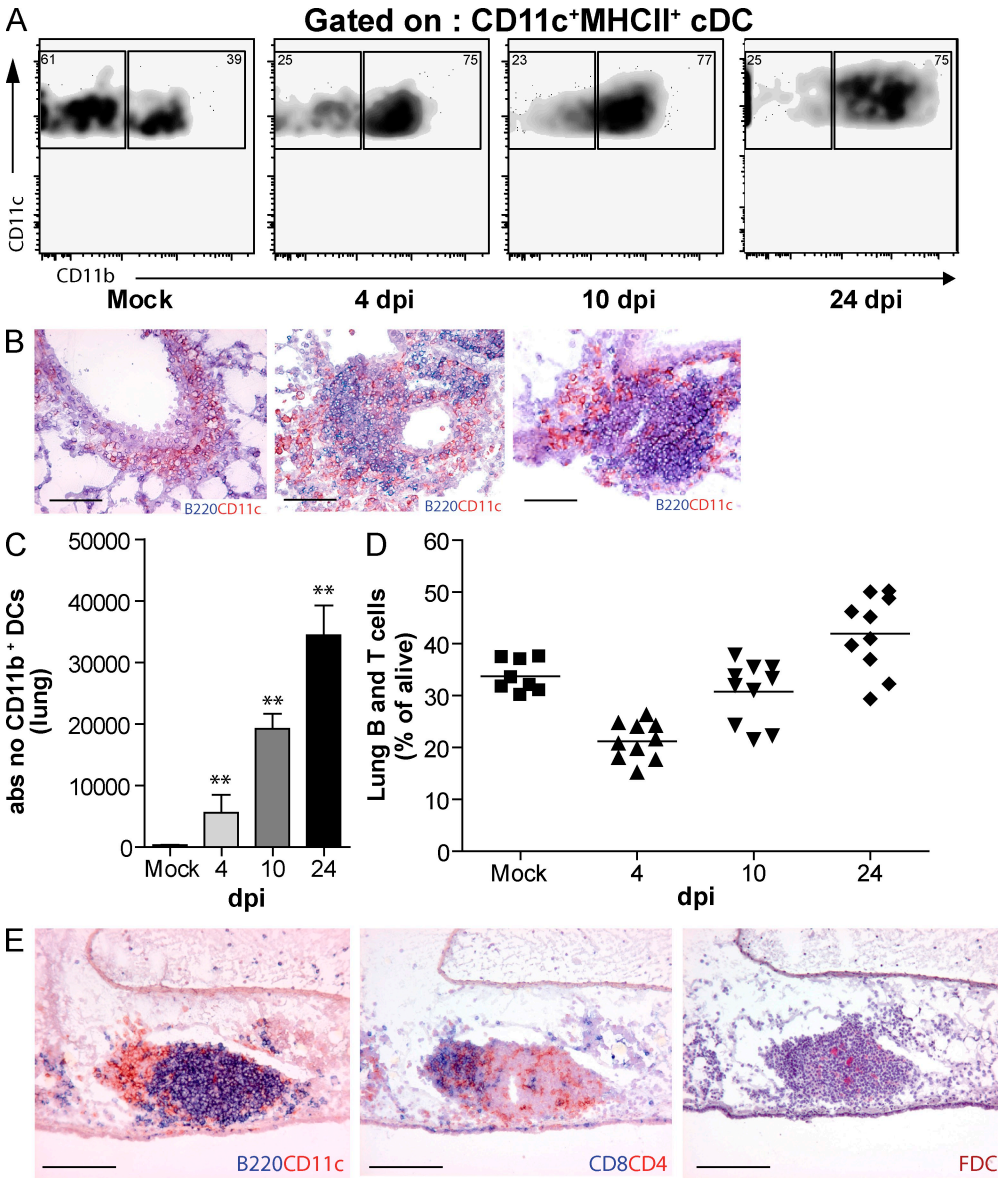

Figure 1. The development of iBALT structures after influenza virus infection. (A) Flow cytometric analysis of CD11b expression on DCs after infection. Numbers in the corners of the plots indicate percentage of MHCII$^+$CD11c$^+$ DCs. (B) Histological slides at 4, 10, and 24 dpi demonstrating B220$^+$ and CD11c$^+$ cells. Bars, 100 µm. (C) Histogram indicates absolute numbers of DC11b$^+$ DCs in lung tissue, bars represent mean values of at least five mice/group, and error bars indicate SEM. **, $P < 0.01$. (D) B and T cells in lung tissue after infection, depicted as percentage of cells alive. Horizontal bars indicate the mean value. (E) Consecutive histological slides from snap-frozen lung tissue at 17 dpi. B220$^+$ B cell structures could be identified, with CD11c$^+$ DCs within the aggregates. Mainly CD4 T cells and some CD8 T cells were present in iBALT and FDCs could be detected. Bars, 100 µm. All results are representative of at least three independent experiments with five animals/group.

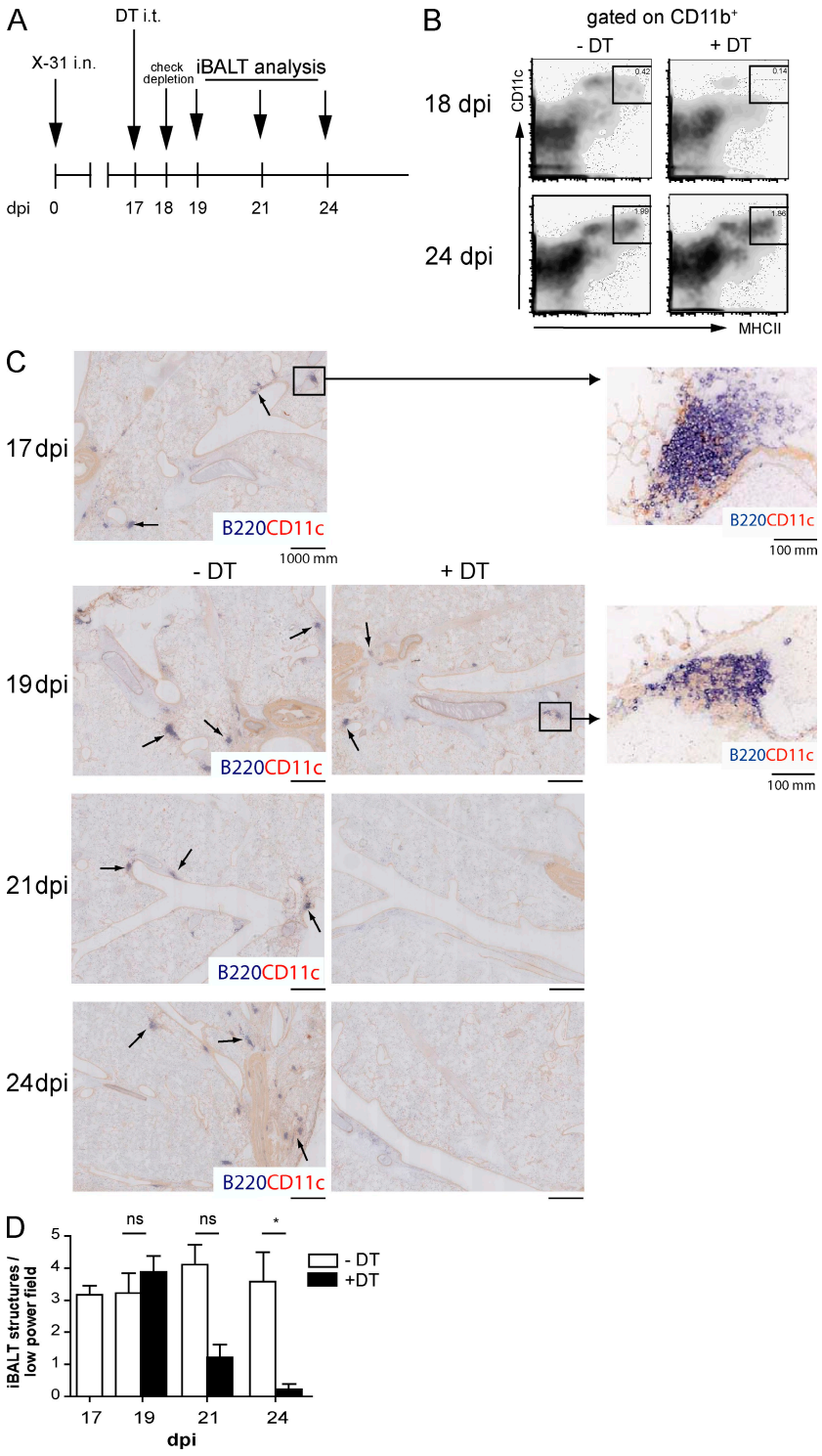

Figure 2. Depletion of CD11c⁺ DCs in a CD11c–DTR mouse model abrogates iBALT structures from the lung. (A) At 17 dpi, mice were treated with DT i.t. and iBALT was analyzed. (B) At 18 dpi and 24 dpi, depletion was checked in lung tissue. At both time points the majority of conventional DCs (cDCs) expressed CD11b. Boxes outline the DC populations, with the numbers indicating mean values of percentage of DCs (of cells alive). (C) At 17 dpi iBALT structures were quantified by a CD11c-B220 staining in a high-power field (top left). B cell clusters are indicated by arrows. A magnification of iBALT in this field is depicted in the inset. At 19, 21, and 24 dpi with and without treatment, B220-CD11c aggregates were depicted on high-power field histology. 2 d after DT treatment (19 dpi), the inset of a B220 follicle demonstrates absence of CD11c⁺ DCs. 1 wk after depletion of CD11c⁺ DCs, dense aggregates could not be detected. (D) Histogram depicts numbers of counted iBALT per low-power field. Bars represent mean values. Three high-power fields were counted per lung of at least five animals per group. Error bars indicate SEM. *, $P < 0.05$. Data are representative of at least two independent experiments.

to identify NP-specific B cells (Fig. S2, B and C). Double staining for NP specificity with the plasma cell marker CD138 confirmed that the majority of NP-specific cells within iBALT were plasma cells (Fig. S2 D). Strikingly, after local depletion of DCs by DT treatment at 17 dpi, these NP-specific plasma cells could no longer be detected on histology 24 dpi (Fig. 3 B). This indicated that besides an abrogation of iBALT aggregates, depletion of DCs seriously affected local immunity. To quantify these changes, multicolor flow cytometry was performed on dispersed lung cells taken 1 wk after DC depletion. The number of total $B220^+CD19^+$ B cells (not depicted) and the number of $B220^+CD19^+$ $IgM^-IgD^-CD95^+$ PNA-positive GC B lymphocytes were significantly decreased (Fig. 3 C). Furthermore, local Ig levels in bronchoalveolar lavage fluid (BALf) were measured. Although the level of class switch–independent IgM remained unaffected by DT treatment, IgA levels were readily decreased (Fig. 3 D). The presence of preserved IgM responses again argues against direct toxic effects of DT on B cells in CD11cDTR Tg mice, as mainly IgM-secreting plasmablasts are sensitive to DT treatment (Hebel et al., 2006). Together, the depletion of $CD11c^+$ DCs pointed out the importance of iBALT structures for the local production of antibodies that rely on GCs for Ig class switching.

Major contribution of iBALT to systemic humoral immunity

The contribution of iBALT plasma cells to systemic humoral immunity has not been studied in great detail. Serum

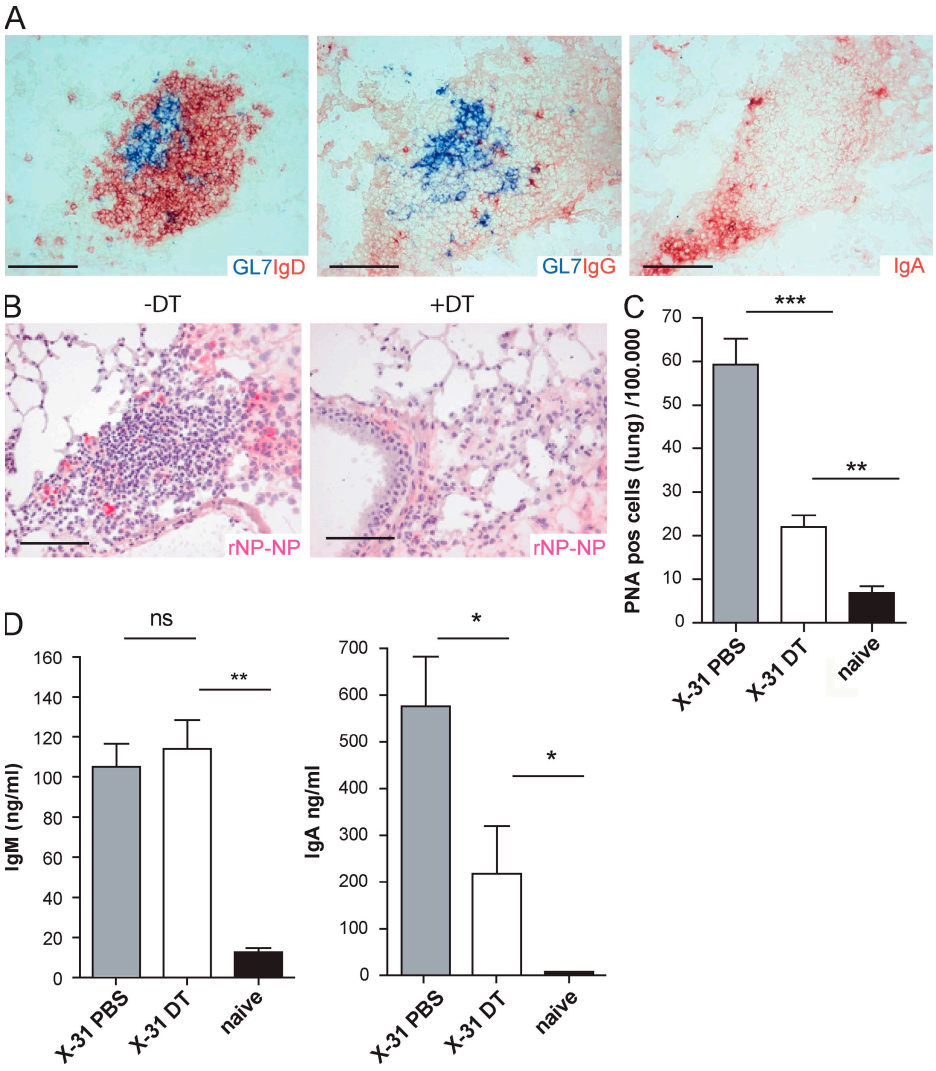

Figure 3. Local humoral immunity is affected by DC depletion. (A) Local class switching in the lung is demonstrated on consecutive slides of lung tissue at 24 dpi that show IgD, IgG, and IgA in the proximity of GL-7 positive GCs. Bars, 100 µm. (B) Depletion of DCs affected presence of NP-specific plasma cells. Bars, 100 µm. (C) Histogram represents the decreased number of $B220^+CD19^+IgM^-IgD^-PNA^+$ cells per 100.000 lung cells 1 wk after DC depletion (DT). (D) Levels of IgM and IgA measured in BALf of mice 1 wk after DC depletion. Bars represent mean values with error bars indicating SEM. All results in this figure represent results of at least five mice per group, and similar results were obtained from at least three separate experiments. *, $P < 0.05$; **, $P < 0.005$; ***, $P < 0.001$.

hemagglutinin (HA)-inhibiting antibodies, the gold standard correlate of protective systemic immunity to influenza, were determined at 24 dpi, 1 wk after DCs and iBALT had been abolished by DT treatment. Surprisingly, the local depletion of DCs and iBALT led to significantly decreased HA-specific antibodies in serum (Fig. 4 A). Although serum virus-specific antibodies may derive from plasma cell production locally in the lung or draining LNs, an important source of serum antibodies are long-lived BM plasma cells (Radbruch et al., 2006). 1 wk after lung DC depletion by DT treatment (24 dpi; Fig. 4 B), $CD19^+CD138^+$ NP-specific plasma cell numbers in BM were found to be significantly decreased. These data suggest that even 17 dpi, the formation of a pool of long-lived plasma cells in the BM depends on continued input of B cells that have undergone class switching in the local TLO of the lung. Because we found that DC depletion leaves the differentiation of NP-specific plasma cells in lung draining LNs intact (Fig. S1, B and C), we conclude that iBALT contributes significantly to systemic humoral immunity. Another possibility was that lung DCs provided a niche for the survival

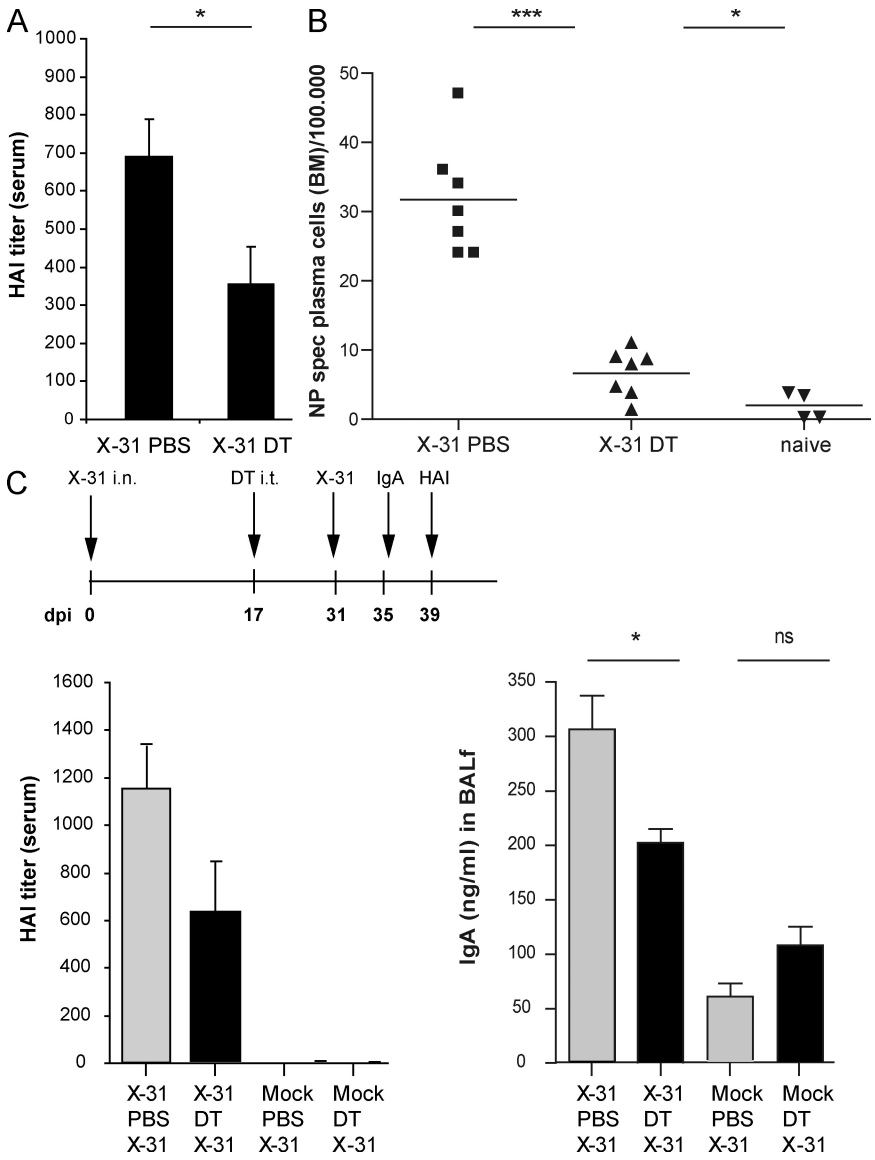

Figure 4. Abrogation of iBALT affected systemic humoral responses. (A) HA inhibition titers measured in serum, indicating the titer of HA-specific antibodies. Mice were treated with DT at 17 dpi and serum was obtained at 24 dpi. Data are representative of three independent experiments with five mice prr group. Bars indicate mean values with error bars indicating SEM. (B) Number of $CD11b^-CD138^+CD95^+NP^+$ plasma cells in BM per 100.000 BM cells. All results in this figure represent results of at least four mice per group, and similar results were obtained from at least three separate experiments. Horizontal bars indicate the mean value. (C) Secondary homologous influenza virus infection 2 wk after DC depletion (DT) or PBS. 4 d after secondary challenge, IgA in BALf was measured (right plot) and 8 d after secondary challenge, HA-inhibiting serum titers were measured (left plot). Bars represent mean values with error bars indicating SEM. All results in this figure represent results of at least five mice per group and similar results were obtained from at least two separate experiments. *, $P < 0.05$; ***, $P < 0.001$; ns, not significant.

of plasma cells in the lung, which subsequently migrated to the BM. In support of this hypothesis, we found significant production of the B cell survival factors BAFF and APRIL by $CD11b^+CD11c^+$ DCs sorted from the lungs of influenza-infected mice but not mock-infected mice (unpublished data). As the DT toxin was given locally to the lungs, we can exclude that the reduction in BM plasma cells was caused by reduction in BM resident DCs, providing a niche for plasma cell survival (Sapoznikov et al., 2008).

To study the biological significance of the decrease in lung and/or BM plasma cells, we reinfected mice with the homologous virus, causing no systemic illness (unpublished data). Mice were infected at day 0 and a second time at day 31. Although reinfection did not cause clinical illness, it strongly boosted serum HA-inhibiting titers and local IgA responses in the BAL fluid when compared with primo-infected mice. However, when iBALT structures were affected by DC depletion intermittently at 17 dpi, reinfection led to lower titers of these antibodies. However, reinfection in DC-depleted mice still elicited stronger humoral immunity when compared with primary infected mice. This was most likely a result of the fact that DC depletion did not fully reduce the pool of long-lived plasma cells in the BM down to the level of noninfected mice (Fig. 4 B), nor did it fully abolish local IgA responses (Fig. 3 D).

After viral clearance, lung $CD11b^+$ DCs no longer present viral antigen yet express homeostatic chemokines

Collectively, our data demonstrated a crucial role for DCs in the maintenance of iBALT structures long after virus had been cleared from the lungs. This could be a result of ongoing presentation of viral antigen by DCs to nearby $CD4^+$ T cells (Fig. 1), which subsequently help in organizing the iBALT structure and local Ig class switching, as has already been suggested for other TLOs (Marinkovic et al., 2006). However, this scenario is less likely, as we studied antigen presentation of viral proteins by $CD11b^+$ DCs at various dpi and found no evidence of antigen presentation to CD4 T cells beyond 4 dpi (Fig. S3).

Previous studies in influenza models indicated that homeostatic chemokines (CCL19, CCL21, and CXCL13) are mainly produced by stromal cells during iBALT formation (Rangel-Moreno et al., 2007). Stromal cells are instructed by a lymphotoxin-$\alpha_1\beta_2$ ($LT\alpha\beta$)–positive cell for this chemokine production. However, studies of the formation of other TLOs have shown that $CD11c^+Ly6C^{lo}$ monocytic precursors to DCs can also be a source of these chemokines and might also provide the $LT\alpha\beta$ to instruct stromal cells (Gräbner et al., 2009). These chemokines, as well as $LT\alpha\beta$, are thought to control both SLO and TLO development by recruiting B cells and retaining plasma cells (CXCL12 and CXCL13) and by attracting T cells (CCL19 and CCL21; Luther et al., 2002; Rangel-Moreno et al., 2007; Gräbner et al., 2009).

To help explain our observations, we studied the expression levels of $LT\alpha\beta$ and homeostatic chemokines in DCs during the maintenance of iBALT. We sorted $CD11c^+CD11b^+$ DCs from digested lung tissue at various dpi (4, 10, and 17 dpi). Importantly, at 17 dpi mRNA expression levels of CXCL12, CXCL13, CCL19, and CCL21, as well as the instructive signal $LT\beta$, were increased in DCs when compared with those at 4 and 10 dpi (Fig. 5 A). We next compared whole lung RNA levels of these factors in uninfected mice and influenza-infected mice at 17 dpi as well as 1 d after DT treatment. Only the instructive $LT\beta$ signal was reduced 1 d after lung DT treatment in CD11c-DTR Tg mice, whereas levels of CXCL13 and CCL21 were unaltered (Fig. 5 B). As at this time point, GCs and B cells were not yet affected (Fig. 2 C) and so the decrease in $LT\beta$ could not be appointed to a loss of B cells. The residual $LT\beta$ signal in DT-treated mice was most likely derived from B cells that still formed aggregates at this time point (Endres et al., 1999). The fact that homeostatic chemokines were intact in whole lungs of DC-depleted mice (but still increased compared with uninfected lungs) suggests that stromal cells were the predominant source of these factors, as has been shown previously (Rangel-Moreno et al., 2007).

As DC depletion led to a loss of preexisting iBALT and was a prominent source of $LT\beta$, we next addressed the functional role of $LT\beta$ receptor signaling in iBALT maintenance. Blocking experiments using $LT\beta R$-Fc given at 17 dpi (Fig. 5 C) led to dissolution of splenic $GL\text{-}7^+$ GC reactions, validating the efficiency of depletion (Rooney et al., 2000). Like DC depletion (Fig. 2), $LT\beta R$-Fc treatment strongly reduced iBALT structures on histology (Fig. 5 C) and the number of $GL\text{-}7^+$ GC B cells when measured by flow cytometry (Fig. 5 C) at 24 dpi. On total lung RNA, $LT\beta R$-Fc treatment led to a strong reduction in CXCL13 levels at 24 dpi, a time point when iBALT structures had disappeared (Fig. 5 D). CCL21 expression however, was not affected by $LT\beta R$-Fc treatment and still increased when compared with naive lungs. As CCL21 is mainly known as a chemoattractant for T cells, a staining for T cells was performed in mice treated with $LT\beta R$-Fc. Although increased T cell numbers were found at 24 dpi in the lungs of $LT\beta R$-Fc–treated infected mice compared with uninfected mice, these cells failed to form the dense clusters seen in isotype-treated infected animals (Fig. S4). A similar effect was seen by depleting DCs in CD11c-DTR mice.

Adoptive transfer of DCs induces iBALT

As a final experiment, we questioned whether adoptive transfer of $CD11b^+$ DCs would also be sufficient to induce iBALT. Therefore, GM-CSF–cultured BM DCs, which are an in vitro equivalent of in vivo inflammatory type $CD11b^+$ DCs, were administered 5× i.t. to naive mice, each with 2-wk intervals. 2 d after the last DC injection, lungs were immunohistochemically stained and examined for the presence of iBALT. Besides $B220^+$ B cell aggregates containing $CD11c^+$ DCs (Fig. 5 E), GCs containing GL-7–positive GC B cells were found, with some IgM or IgG antibody-secreting plasma cells. These findings indicate that DCs may well exert their effects on TLO neogenesis directly. However, because we have previously shown that adoptive transfer of DCs to the

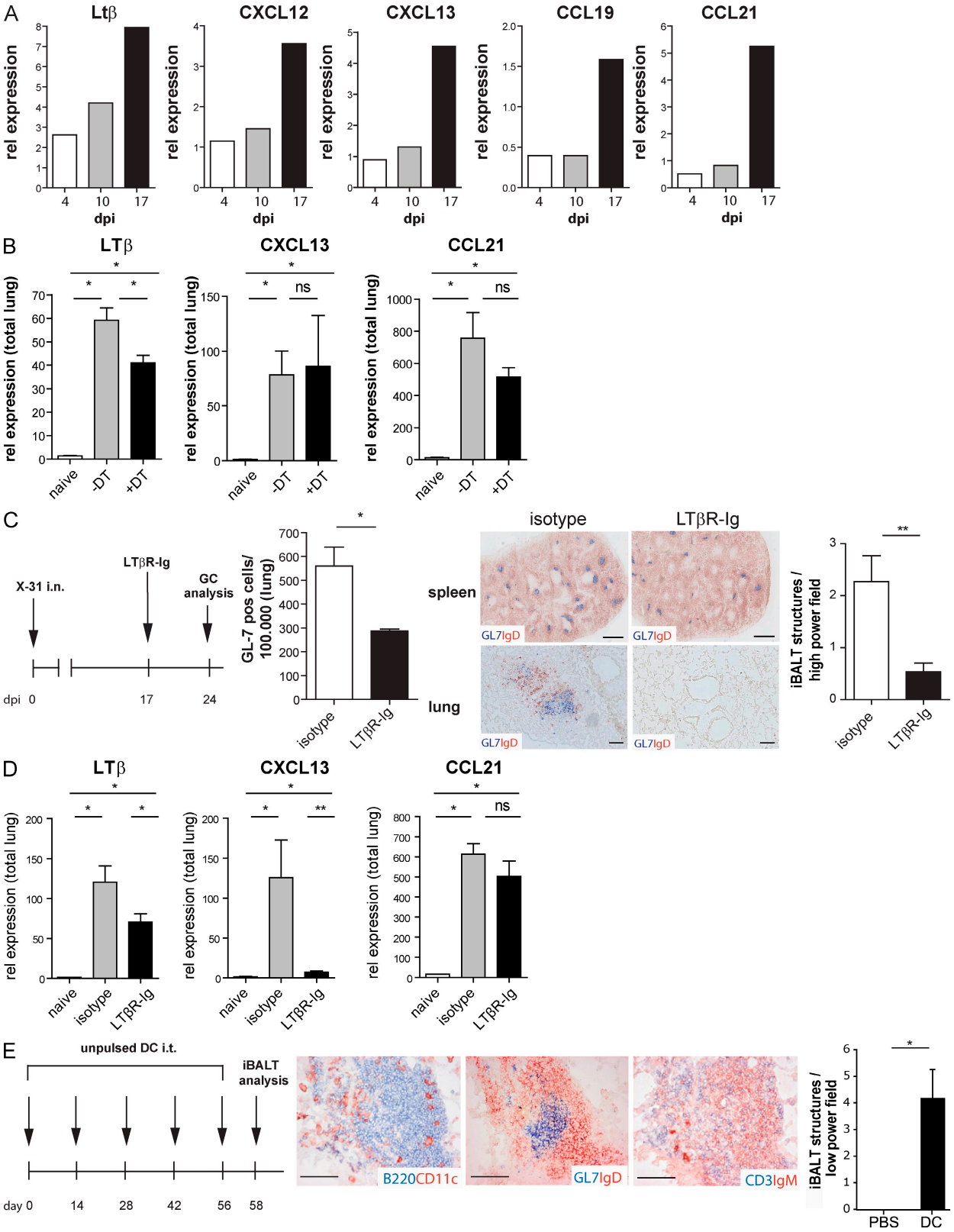

Figure 5. DCs are capable of maintaining iBALT as a result of chemokine expression. (A) Relative expression of lymphotoxin-β, CXCL12, CXCL13, CCL19, and CCL21 on sorted CD11b$^+$ DCs obtained from pooled lung tissues of 10 infected mice at various dpi. Bars indicate relative expression. (B) Relative expression of lymphotoxin-β, CXCL13, and CCL21 on total lung RNA of naive mice and with or without DT treatment. Bars represent mean values of five mice per group with error bars indicating SEM. *, $P < 0.05$; ns, not significant. (C) Mice infected at day 0 were treated with LTβR-Fc or an isotype at

lungs causes airway inflammation (Lambrecht et al., 2000a) it is also conceivable these effects on TLO neogenesis are induced via chronic inflammation. However, in a chronic lung inflammation model using chronic OVA aerosol exposure for equally long time periods, we failed to detect significant iBALT structures (unpublished data).

Concluding remarks

Previous work on the role of iBALT structures in mediating immunity to influenza have all used genetic targeting strategies that led to deficiencies of SLO in addition to TLO, potentially overemphasizing the contribution of iBALT to antiviral immunity (Moyron-Quiroz et al., 2004). Using the induced depletion of DCs to eliminate iBALT, but not SLO, we were able to demonstrate a clear role for these structures in both local and systemic humoral immunity to influenza virus.

A big question that remains in the field of ectopic lymphoid tissue development is the precise character of the LTβ$^+$ lymphoid tissue inducer cells that provide the initial trigger for TLO development to stromal organizer cells (Marinkovic et al., 2006). As we have studied the maintenance of TLO in the lung, our paper does not answer this question but provides clear evidence that DCs play a crucial role in the organization and maintenance of established TLO. We suggest a model by which the CD11b$^+$ DC maintains TLO by providing a continued source of LTβ that is necessary for maintaining high levels CXCL13 and retention of B cells inside the TLO structure. Although DCs can be a direct source of homeostatic chemokines, most likely stromal cells are quantitatively more important (Rangel-Moreno et al., 2007). However, in the induced absence of DCs or under conditions of LTβR blockade, continued production of homeostatic chemokines by stromal cells is not sufficient for maintaining the iBALT structure. One possibility that remains to be elucidated is that DCs are crucial for the correct positioning of stromal-derived homeostatic chemokines. By binding and displaying stromal-derived chemokines on their surface, DCs could retain T cells and B cells in dense clusters, which are necessary for GC reactions and immunoglobulin class switching.

MATERIALS AND METHODS

Mice. C57BL/6 mice (6–8 wk) were purchased from Harlan Laboratories. The generation and screening of CD11c-DTR Tg mice has been reported previously (Jung et al., 2002). Male BALB/c background CD11c-DTR Tg (H2-D^d) mice were crossed with C57BL/6 (H2-D^b) to obtain F1 progeny. CD11c^{hi} cells were depleted in CD11c-DTR x C57BL/6 Tg mice by i.t. injection of 50 ng DT, a dose previously determined by titration. All experiments were approved by an independent animal ethics committee of Erasmus MC Medical Center (Rotterdam, Netherlands).

Influenza virus infection. Mice were intranasally infected with 10^5 $TCID_{50}$ H3N2 influenza virus X-31 (Medical Research Council) diluted in 50 μl PBS. For antigen presentation assays of lung DCs, mice were infected with 10^5 X-31 influenza virus encoding $OVA_{323-339}$ MHC II epitope in HA of the virus (Thomas et al., 2006). The OVA virus was provided by R. Webby (St. Jude Children's Hospital, Memphis, TN). In some experiments, mice were treated at 17 dpi with 200 μg/mouse LTβR-Fc (provided by C.F. Ware, La Jolla Institute for Allergy and Immunology, San Diego, CA).

Histology. Lungs were inflated with OCT, snap frozen in liquid nitrogen, and stored at −80°C. Frozen sections were fixed in acetone and endogenic peroxidase was blocked before immunohistochemical staining. Immunohistochemical double staining was performed for B220 (RA3-6B2; BD) and CD11c (N418; eBioscience), CD8 (KT-15; AbD Serotec) and CD4 (RM4-5; eBioscience), GL7 (BD) and IgD (eBioscience), IgG (A85-1; BD) and PNA (L-6135; Sigma-Aldrich), IgA (02262D; BD) and PNA, and IgM (II-41; BD) and KT3 (supernatant). FDC (M2; BD) was single stained. For detection of NP-positive cells, slides were incubated with recombinant NP (Voeten et al., 1998) before FITC-labeled anti-NP staining. Slides were digitized on a Digital Zoom Microscope (Hamamatsu). All depicted pictures are representative of at least five mice per group. Quantification of iBALT was performed by counts of the number of GL-7–positive structures per high-power field. Three high-power fields were counted per lung of at least five mice per group.

Detection of antibodies in serum and BALf. For detection of HA-specific antibodies in serum, samples were treated with cholera filtrate and heat inactivated at 56°C. The serum samples were tested for the presence of anti-HA antibodies. For this purpose, an HA inhibition assay was used according to a standard protocol of 1% turkey erythrocytes and 4 HA units of H3N2 influenza virus (Masurel et al., 1981) in 96-wells plates (Greiner Bio-One). ELISA was performed on BALf for detection of IgA (BD) and IgM (SouthernBiotech).

Adoptive transfer of GM-CSF–cultured DCs. BM cells were cultured for 9 d in DC culture medium (DC-TCM; RPMI 1640 containing GlutaMAX-I [Invitrogen] supplemented with 5% [vol/vol] FCS [Sigma-Aldrich], 50 μM 2-mercaptoethanol [Sigma-Aldrich], 50 μg/ml gentamicin [Invitrogen], and 20 ng/ml of recombinant mouse GM-CSF [gift from K. Thielemans, Vrije Universiteit Brussel, Brussels, Belgium]). Mice received five i.t. injections of 10^6 DCs, each with a 2-wk interval.

Flow cytometry and cell sorting. To check the depletion of cell subsets after treatment with DT and analyze tissues after depletion, single cell suspensions of lung and BM were prepared as described previously (de Heer et al., 2004). Extracellular staining for DCs was done by staining with 120G8 FITC (provided by C. Asselin-Paturel, Schering-Plough Laboratory for Immunological Research, Dardilly, France), CD11b PE, MHCII PECy5, B220

17 dpi and analyzed 24 dpi. The left histogram represents GL-7–positive cells in lung tissue measured by flow cytometry, with bars representing mean values of five mice per group and error bars indicating SEM. *, $P < 0.05$. Histology of spleen (top) and lung (bottom) demonstrate high-power field images of GL7-IgD aggregates after treatment with LTβR-Fc or an isotype, representative of at least five mice per group. Bars, 1,000 μm. The right histogram demonstrates numbers of counted iBALT/high-power field. Bars represent mean values of three high-power fields counted per lung of at least five animals per group. Error bars indicate SEM. **, $P < 0.01$. (D) Relative expression of lymphotoxin-β, CXCL13, and CCL21 on total lung RNA of naive mice and 1 wk after LTβR-Fc or isotype treatment. Bars represent mean values of five mice per group with error bars indicating SEM. *, $P < 0.05$; **, $P < 0.005$; ns, not significant. (E) Repetitive adoptive transfer of cultured GM-CSF DCs induced iBALT. DCs were grown from BM and injected five times with 2-wk intervals as a control PBS was injected. Consecutive histological slides show presence of iBALT aggregates. Bars, 100 μm. The histogram demonstrates numbers of counted iBALT per high-power field. Bars represent mean values of three low-power fields counted per lung of at least five animals per group. Error bars indicate SEM. *, $P < 0.05$. All experiments in this figure have been independently performed twice with at least five mice per group.

PECy7(eBioscience), CD11c PETxR(Invitrogen), CD3 APC Cy7, CD19 APC Cy7 (BD), and a live/dead marker (DAPI) in violet. PNA-positive GCs in lung were detected with mAbs against IgD FITC, CD95 PE, IgM PECy7, B220 AF700 (BD), CD19 PerCp Cy5.5 (eBioscience), biotinylated PNA (Sigma-Aldrich), and DAPI. For detection of NP-specific plasma cells in BM, cells were first stained extracellularly with CD138 PE (BD), CD19 PerCp Cy5.5, CD11b AF700 (eBioscience), and an Aqua Live/Dead marker (Invitrogen). Next, Cytofix/Cytoperm (BD) was added to fixate cells. Recombinant NP was diluted in perm buffer and added to each well. Cells were incubated for 30 min and then washed with perm buffer. Intracellular cells were stained with NP FITC (Dako), IgM APC, biotinylated IgG2a/2b (BD), and secondary streptavidin APC Cy7 (eBioscience). Acquisition of 10-color samples was performed on a cytometer (LSR) equipped with FACSDiva software (both BD). Final analysis and graphical output were performed using FlowJo software (Tree Star, Inc.). For sorting of DCs, mice were sacrificed at different time points after infection with X-31 influenza virus. Lungs of 10 animals were pooled and digested in a collagenase-DNase solution for 1 h at 37°C to promote release of DCs. DCs were stained as described in this section and cell sorting was performed on a FACSAria. The purity of sorted populations was >98%.

Antigen presentation assay. For the coculture of sorted DC subsets with OVA-specific $CD4^+$ T cells, OT-2 transgenic T cells were isolated from the spleen and MLN of an OT-2 mouse, enriched by MACS cell sorting with anti-CD4 antibodies according to the manufacturer's protocol (Miltenyi Biotec), and labeled with CFSE (Lambrecht et al., 2000b). Sorted DC subsets were cocultured with T cells in a v-bottom plate at a 1/10 ratio for 4 d. T cell divisions were measured by flow cytometry on an LSR cytometer equipped with FACSDiva software (both from BD). Supernatant was stored at −20°C.

Real-time quantitative RT-PCR. Quantative RT-PCR for CCL19, CCL21, CXCL12, CXCL13, and LTβ was performed on RNA obtained from sorted lung DC subsets. RNA was isolated with RNAqueous micro kit (Applied Biosystems) and treated with DNase I, according to the manufacturer's protocol. 100 ng RNA was reverse transcribed using Superscript II (Invitrogen) and random hexamers (GE Healthcare) for 50 min at 42°C. Quantitative PCR was performed with Taqman Universal PCR MasterMix (Applied Biosystems) and preformulated primers and probe mixes (Assay on Demand; Applied Biosystems). PCR conditions were 2 min at 50°C and 10 min at 95°C, followed by 40 cycles of 15 s at 95°C and 60°C for 1 min using an ABI PRISM 7300 (Applied Biosystems). PCR amplification of the housekeeping gene encoding ubiquitin C was performed during each run for each sample to allow normalization between samples.

Statistical analysis. All experiments were performed using 5–10 animals per group. All experiments were performed at least two to three times. The difference between groups was calculated using the Mann-Whitney *U* test for unpaired data (Prism version 4.0; GraphPad Software, Inc.). Differences were considered significant when $P < 0.05$.

Online supplemental material. Fig. S1 depicts the effect of DT treatment on various cell populations in MLN and lung tissue. Fig. S2 depicts histological analysis of iBALT. Fig. S3 shows CFSE proliferation plots of T cells stimulated with DCs sorted from lungs at 4 and 17 dpi with a virus containing an OVA epitope. Fig. S4 demonstrates the effect of DT and LTβRIg treatment on CD4CD8 T cell areas in iBALT. Online supplemental material is available at http://www.jem.org/cgi/content/full/jem.20090410/DC1.

C.H. Geurtsvankessel is supported by a VIRGO grant from the Dutch Organization for Scientific Research. B.N. Lambrecht is supported by an Odysseus Grant of the Flemish Government and by a VIRGO grant of the Dutch Organization for Scientific Research.

The authors have no conflicting financial interests.

Submitted: 23 February 2009
Accepted: 1 September 2009

REFERENCES

Aloisi, F., and R. Pujol-Borrell. 2006. Lymphoid neogenesis in chronic inflammatory diseases. *Nat. Rev. Immunol.* 6:205–217. doi:10.1038/nri1786

Banchereau, J., and R.M. Steinman. 1998. Dendritic cells and the control of immunity. *Nature.* 392:245–252. doi:10.1038/32588

Beaty, S.R., C.E. Rose Jr., and S.S. Sung. 2007. Diverse and potent chemokine production by lung CD11bhigh dendritic cells in homeostasis and in allergic lung inflammation. *J. Immunol.* 178:1882–1895.

Cupedo, T., and R.E. Mebius. 2005. Cellular interactions in lymph node development. *J. Immunol.* 174:21–25.

Cupedo, T., W. Jansen, G. Kraal, and R.E. Mebius. 2004. Induction of secondary and tertiary lymphoid structures in the skin. *Immunity.* 21:655–667. doi:10.1016/j.immuni.2004.09.006

de Heer, H.J., H. Hammad, T. Soullié, D. Hijdra, N. Vos, M.A. Willart, H.C. Hoogsteden, and B.N. Lambrecht. 2004. Essential role of lung plasmacytoid dendritic cells in preventing asthmatic reactions to harmless inhaled antigen. *J. Exp. Med.* 200:89–98. doi:10.1084/jem.20040035

Drayton, D.L., S. Liao, R.H. Mounzer, and N.H. Ruddle. 2006. Lymphoid organ development: from ontogeny to neogenesis. *Nat. Immunol.* 7:344–353. doi:10.1038/ni1330

Endres, R., M.B. Alimzhanov, T. Plitz, A. Fütterer, M.H. Kosco-Vilbois, S.A. Nedospasov, K. Rajewsky, and K. Pfeffer. 1999. Mature follicular dendritic cell networks depend on expression of lymphotoxin β receptor by radioresistant stromal cells and of lymphotoxin β and tumor necrosis factor by B cells. *J. Exp. Med.* 189:159–168. doi:10.1084/jem.189.1.159

GeurtsvanKessel, C.H., and B.N. Lambrecht. 2008. Division of labor between dendritic cell subsets of the lung. *Mucosal Immunol.* 1:442–450. doi:10.1038/mi.2008.39

GeurtsvanKessel, C.H., M.A. Willart, L.S. van Rijt, F. Muskens, M. Kool, C. Baas, K. Thielemans, C. Bennett, B.E. Clausen, H.C. Hoogsteden, et al. 2008. Clearance of influenza virus from the lung depends on migratory langerin$^+$CD11b$^-$ but not plasmacytoid dendritic cells. *J. Exp. Med.* 205:1621–1634. doi:10.1084/jem.20071365

Gräbner, R., K. Lötzer, S. Döpping, M. Hildner, D. Radke, M. Beer, R. Spanbroek, B. Lippert, C.A. Reardon, G.S. Getz, et al. 2009. Lymphotoxin β receptor signaling promotes tertiary lymphoid organogenesis in the aorta adventitia of aged *ApoE*$^{-/-}$ mice. *J. Exp. Med.* 206:233–248. doi:10.1084/jem.20080752

Hebel, K., K. Griewank, A. Inamine, H.D. Chang, B. Müller-Hilke, S. Fillatreau, R.A. Manz, A. Radbruch, and S. Jung. 2006. Plasma cell differentiation in T-independent type 2 immune responses is independent of CD11c(high) dendritic cells. *Eur. J. Immunol.* 36:2912–2919. doi:10.1002/eji.200636356

Hogg, J.C., F. Chu, S. Utokaparch, R. Woods, W.M. Elliott, L. Buzatu, R.M. Cherniack, R.M. Rogers, F.C. Sciurba, H.O. Coxson, and P.D. Paré. 2004. The nature of small-airway obstruction in chronic obstructive pulmonary disease. *N. Engl. J. Med.* 350:2645–2653. doi:10.1056/NEJMoa032158

Jung, S., D. Unutmaz, P. Wong, G. Sano, K. De los Santos, T. Sparwasser, S. Wu, S. Vuthoori, K. Ko, F. Zavala, et al. 2002. In vivo depletion of CD11c(+) dendritic cells abrogates priming of CD8(+) T cells by exogenous cell-associated antigens. *Immunity.* 17:211–220. doi:10.1016/S1074-7613(02)00365-5

Kendall, P.L., G. Yu, E.J. Woodward, and J.W. Thomas. 2007. Tertiary lymphoid structures in the pancreas promote selection of B lymphocytes in autoimmune diabetes. *J. Immunol.* 178:5643–5651.

Kocks, J.R., A.C. Davalos-Misslitz, G. Hintzen, L. Ohl, and R. Förster. 2007. Regulatory T cells interfere with the development of bronchus-associated lymphoid tissue. *J. Exp. Med.* 204:723–734. doi:10.1084/jem.20061424

Kratz, A., A. Campos-Neto, M.S. Hanson, and N.H. Ruddle. 1996. Chronic inflammation caused by lymphotoxin is lymphoid neogenesis. *J. Exp. Med.* 183:1461–1472. doi:10.1084/jem.183.4.1461

Lambrecht, B.N., M. De Veerman, A.J. Coyle, J.C. Gutierrez-Ramos, K. Thielemans, and R.A. Pauwels. 2000a. Myeloid dendritic cells induce Th2 responses to inhaled antigen, leading to eosinophilic airway inflammation. *J. Clin. Invest.* 106:551–559. doi:10.1172/JCI8107

Lambrecht, B.N., R.A. Pauwels, and B. Fazekas De St Groth. 2000b. Induction of rapid T cell activation, division, and recirculation by intratracheal

injection of dendritic cells in a TCR transgenic model. *J. Immunol.* 164:2937–2946.

Luther, S.A., A. Bidgol, D.C. Hargreaves, A. Schmidt, Y. Xu, J. Paniyadi, M. Matloubian, and J.G. Cyster. 2002. Differing activities of homeostatic chemokines CCL19, CCL21, and CXCL12 in lymphocyte and dendritic cell recruitment and lymphoid neogenesis. *J. Immunol.* 169:424–433.

Magliozzi, R., S. Columba-Cabezas, B. Serafini, and F. Aloisi. 2004. Intracerebral expression of CXCL13 and BAFF is accompanied by formation of lymphoid follicle-like structures in the meninges of mice with relapsing experimental autoimmune encephalomyelitis. *J. Neuroimmunol.* 148:11–23. doi:10.1016/j.jneuroim.2003.10.056

Marinkovic, T., A. Garin, Y. Yokota, Y.X. Fu, N.H. Ruddle, G.C. Furtado, and S.A. Lira. 2006. Interaction of mature CD3+CD4+ T cells with dendritic cells triggers the development of tertiary lymphoid structures in the thyroid. *J. Clin. Invest.* 116:2622–2632.

Masurel, N., P. Ophof, and P. de Jong. 1981. Antibody response to immunization with influenza A/USSR/77 (H1N1) virus in young individuals primed or unprimed for A/New Jersey/76 (H1N1) virus. *J. Hyg. (Lond.).* 87:201–209.

Moyron-Quiroz, J.E., J. Rangel-Moreno, K. Kusser, L. Hartson, F. Sprague, S. Goodrich, D.L. Woodland, F.E. Lund, and T.D. Randall. 2004. Role of inducible bronchus associated lymphoid tissue (iBALT) in respiratory immunity. *Nat. Med.* 10:927–934. doi:10.1038/nm1091

Moyron-Quiroz, J.E., J. Rangel-Moreno, L. Hartson, K. Kusser, M.P. Tighe, K.D. Klonowski, L. Lefrançois, L.S. Cauley, A.G. Harmsen, F.E. Lund, and T.D. Randall. 2006. Persistence and responsiveness of immunologic memory in the absence of secondary lymphoid organs. *Immunity.* 25:643–654. doi:10.1016/j.immuni.2006.08.022

Nasr, I.W., M. Reel, M.H. Oberbarnscheidt, R.H. Mounzer, F.K. Baddoura, N.H. Ruddle, and F.G. Lakkis. 2007. Tertiary lymphoid tissues generate effector and memory T cells that lead to allograft rejection. *Am. J. Transplant.* 7:1071–1079. doi:10.1111/j.1600-6143.2007.01756.x

Radbruch, A., G. Muehlinghaus, E.O. Luger, A. Inamine, K.G. Smith, T. Dörner, and F. Hiepe. 2006. Competence and competition: the challenge of becoming a long-lived plasma cell. *Nat. Rev. Immunol.* 6:741–750. doi:10.1038/nri1886

Rangel-Moreno, J., L. Hartson, C. Navarro, M. Gaxiola, M. Selman, and T.D. Randall. 2006. Inducible bronchus-associated lymphoid tissue (iBALT) in patients with pulmonary complications of rheumatoid arthritis. *J. Clin. Invest.* 116:3183–3194. doi:10.1172/JCI28756

Rangel-Moreno, J., J.E. Moyron-Quiroz, L. Hartson, K. Kusser, and T.D. Randall. 2007. Pulmonary expression of CXC chemokine ligand 13, CC chemokine ligand 19, and CC chemokine ligand 21 is essential for local immunity to influenza. *Proc. Natl. Acad. Sci. USA.* 104:10577–10582. doi:10.1073/pnas.0700591104

Rooney, I., K. Butrovich, and C.F. Ware. 2000. Expression of lymphotoxins and their receptor-Fc fusion proteins by baculovirus. *Methods Enzymol.* 322:345–363. doi:10.1016/S0076-6879(00)22032-6

Sapoznikov, A., J.A. Fischer, T. Zaft, R. Krauthgamer, A. Dzionek, and S. Jung. 2007. Organ-dependent in vivo priming of naive $CD4^+$, but not $CD8^+$, T cells by plasmacytoid dendritic cells. *J. Exp. Med.* 204:1923–1933. doi:10.1084/jem.20062373

Sapoznikov, A., Y. Pewzner-Jung, V. Kalchenko, R. Krauthgamer, I. Shachar, and S. Jung. 2008. Perivascular clusters of dendritic cells provide critical survival signals to B cells in bone marrow niches. *Nat. Immunol.* 9:388–395. doi:10.1038/ni1571

Thomas, P.G., S.A. Brown, W. Yue, J. So, R.J. Webby, and P.C. Doherty. 2006. An unexpected antibody response to an engineered influenza virus modifies CD8+ T cell responses. *Proc. Natl. Acad. Sci. USA.* 103:2764–2769. doi:10.1073/pnas.0511185103

Tsuji, M., K. Suzuki, H. Kitamura, M. Maruya, K. Kinoshita, I.I. Ivanov, K. Itoh, D.R. Littman, and S. Fagarasan. 2008. Requirement for lymphoid tissue-inducer cells in isolated follicle formation and T cell-independent immunoglobulin A generation in the gut. *Immunity.* 29:261–271. doi:10.1016/j.immuni.2008.05.014

van Rijt, L.S., S. Jung, A. Kleinjan, N. Vos, M. Willart, C. Duez, H.C. Hoogsteden, and B.N. Lambrecht. 2005. In vivo depletion of lung $CD11c^+$ dendritic cells during allergen challenge abrogates the characteristic features of asthma. *J. Exp. Med.* 201:981–991. doi:10.1084/jem.20042311

Voeten, J.T., J. Groen, D. van Alphen, E.C. Claas, R. de Groot, A.D. Osterhaus, and G.F. Rimmelzwaan. 1998. Use of recombinant nucleoproteins in enzyme-linked immunosorbent assays for detection of virus-specific immunoglobulin A (IgA) and IgG antibodies in influenza virus A- or B-infected patients. *J. Clin. Microbiol.* 36:3527–3531.